

Supplementary Information

The role of ultra-thin MnO_x co-catalysts on the photoelectrochemical properties of BiVO_4 photoanodes

Rowshanak Irani¹, Paul Plate¹, Christian Höhn¹, Peter Bogdanoff¹, Markus Wollgarten¹, Katja Höflich¹,
Roel van de Krol¹, Fatwa F. Abdi^{1,*}

¹ Institute for Solar Fuels, Helmholtz-Zentrum Berlin für Materialien und Energie GmbH, Hahn-Meitner-
Platz 1, Berlin 14109, Germany

* correspondence: fatwa.abdi@helmholtz-berlin.de

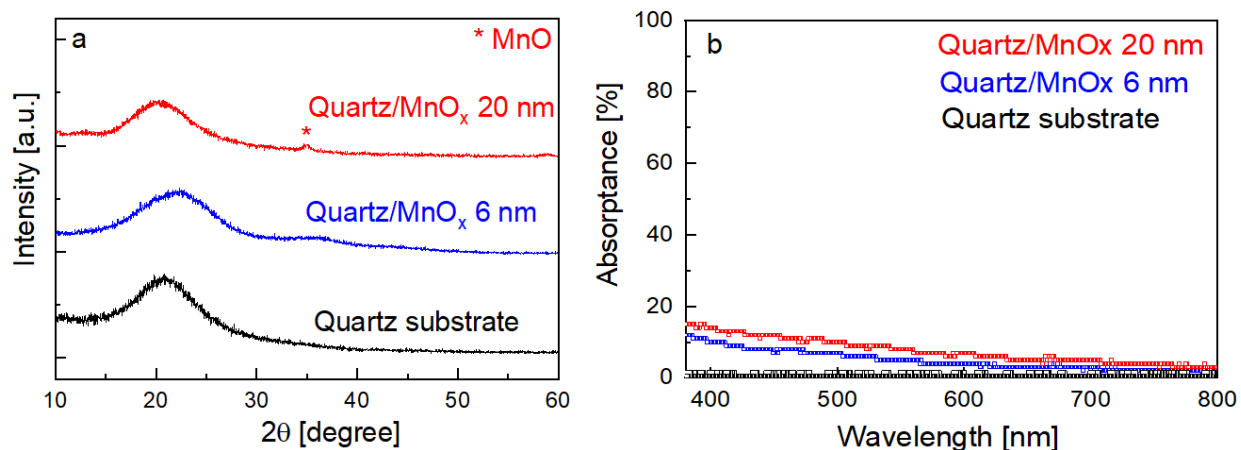


Figure S1. **a)** X-ray diffractograms for the quartz substrate and MnO_x samples deposited on quartz (6 and 20 nm). **b)** The absorbance of the quartz substrate and different thicknesses of MnO_x (6 and 20 nm) deposited on quartz.

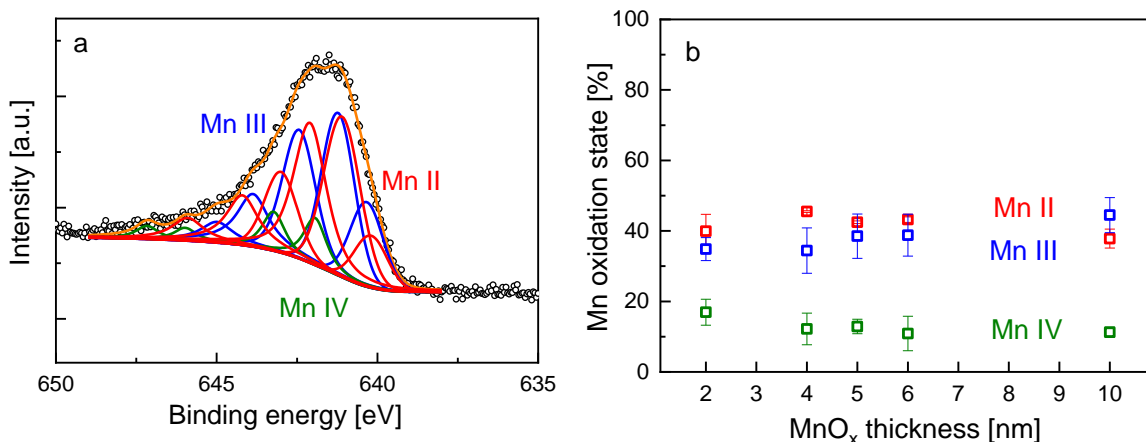


Figure S2. a) A fitting example of Mn $2p_{3/2}$ core-level peak to quantify the manganese oxidation states in $\text{BiVO}_4/\text{MnO}_x$ 4 nm, based on the fitting procedure described in Biesinger et al. *Appl. Surf. Sci.* **257**, 2011, 2717-2730. b) The oxidation states of the MnO_x films with different thicknesses. Mn^{2+} , Mn^{3+} , and Mn^{4+} are present in all of the samples with similar percentages regardless of the thickness.

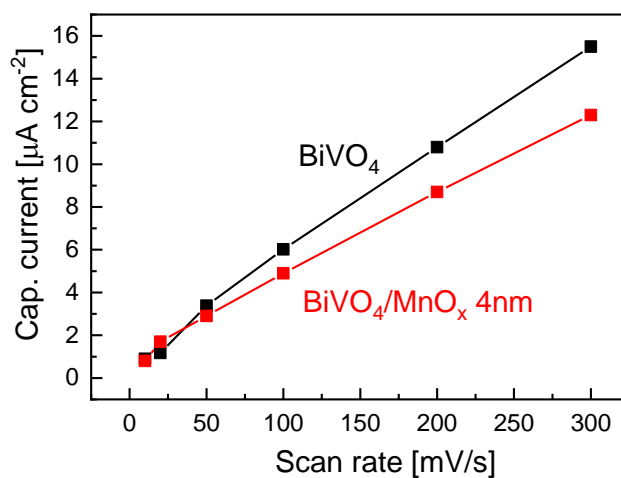


Figure S3. Capacitive current density of the BiVO_4 and $\text{BiVO}_4/\text{MnO}_x$ (4 nm) films as a function of the applied potential scan rate. The ratio of the slope of these curves represents the ratio of the electrochemically active surface area (ECSA) of the films.

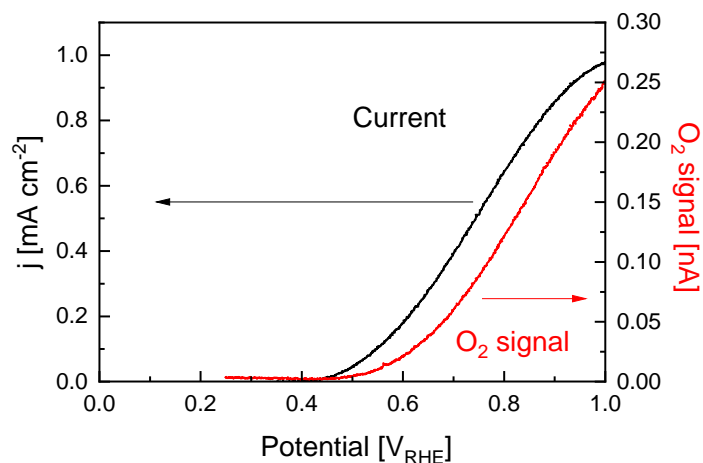


Figure S4. Electrochemical mass spectrometry (EMS) data obtained during LSV scans of the BiVO₄/MnO_x (4 nm) photoanode. The current density is shown in black and the O₂ signal in red. Measurements were done in 0.5 M KP_i (pH ~7) under back illumination with a scan rate of 2 mV/s. The slight delay between the current and the O₂ signal is due to the time it takes for the O₂ molecules to diffuse from the surface of the photoanode to the mass spectrometer.

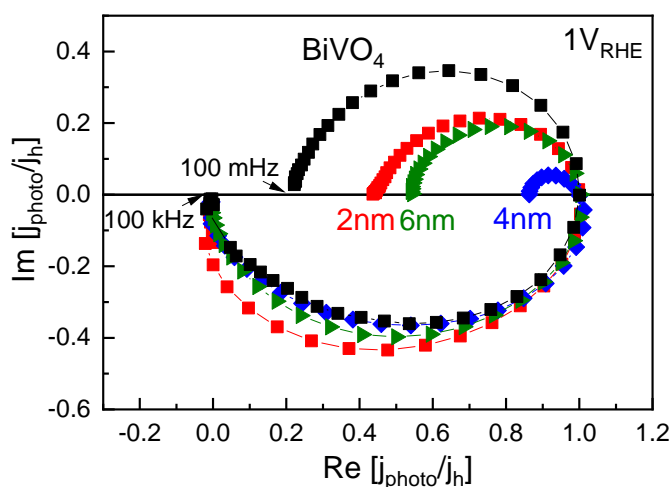


Figure S5. IMPS spectra of bare BiVO₄ photoanode and BiVO₄ coated with different thicknesses of MnO_x co-catalyst (2, 4, 6 nm) under 1 V_{RHE} applied potentials.

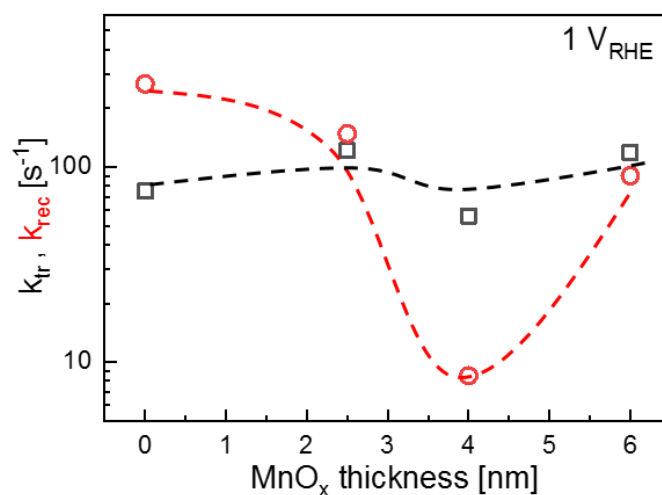


Figure S6. Charge transfer (k_{tr}) and surface recombination (k_{rec}) rate constants for BiVO_4 samples with different thicknesses of MnO_x co-catalyst at 1 V vs. RHE. The dash line is added as a guide to the eye.

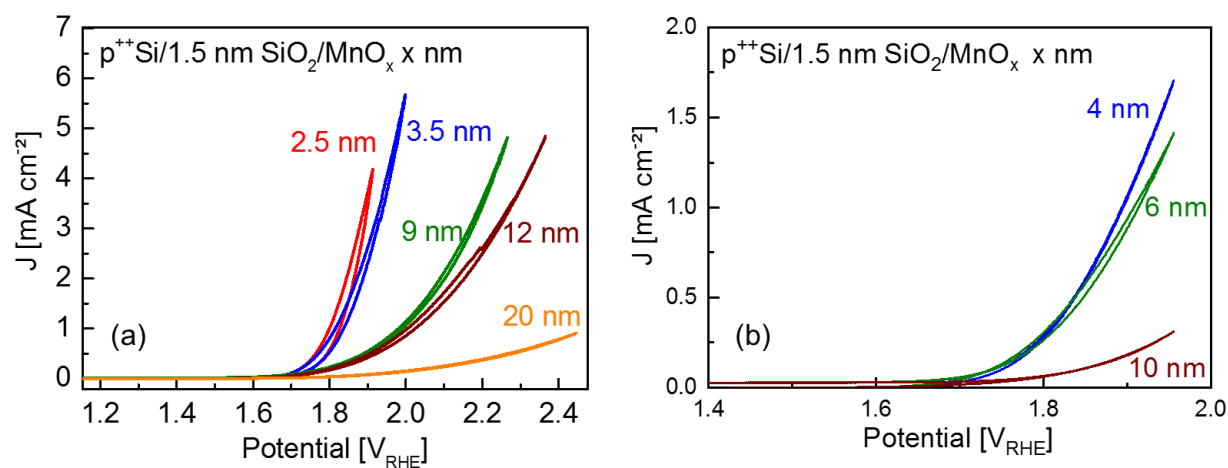


Figure S7. Cyclic voltammogram of MnO_x films with different thicknesses on $\text{p}^{++}\text{Si}/1.5 \text{ nm SiO}_2$ substrate measured in (a) 0.1 M KOH and (b) 0.1 M KP_i electrolyte (pH ~ 7). The measurement was taken with a scan rate of 10 mV/s .

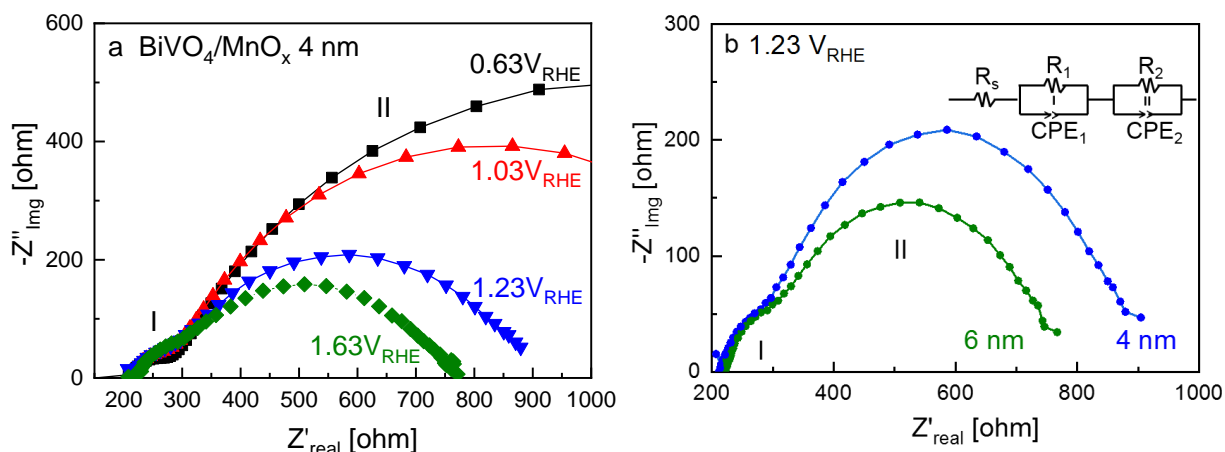


Figure S8. a) Nyquist plots for EIS data measured for 4 nm MnO_x coated BiVO_4 in KP_i (pH~7.38). Various potentials have been applied (0.63, 1.03, 1.23, and 1.63 V vs. RHE). **b)** A comparison between the Nyquist plot of the 4 and 6 nm MnO_x in $\text{BiVO}_4/\text{MnO}_x$ system at 1.23 V vs. RHE. Both experiments were performed under a 455 nm LED with 20 mWcm^{-2} power density. The inset shows the equivalent circuit which was employed for fitting.

Table S1. The extent of band bending in our BiVO_4 films with various thicknesses of MnO_x , as calculated from the difference of our measured XPS core-level peak position (i.e., surface, E^S) and the corresponding peak position in the bulk (E^B); $E_{\text{band bending extend (bb)}} = E^B - E^S$. The binding energies of the single crystal BiVO_4 are assumed to be valid for the bulk, which were reported to be 159.3 and 516.9 eV for Bi $4f_{7/2}$ and V $2p_{3/2}$, respectively (Favaro et al. *J. Phys. Chem. C* **123**, 2019, 8347-8359).

MnO_x thickness (nm)	$E_{\text{Bi } 4f}^S$ (eV)	$E_{\text{V } 2p}^S$ (eV)	$E_{bb}^{\text{Bi } 4f} = E^B - E^S$ (eV)	$E_{bb}^{\text{V } 2p} = E^B - E^S$ (eV)
0	159.00	516.70	0.30	0.20
2	158.95	516.65	0.35	0.25
4	158.95	516.60	0.35	0.30
5	158.85	516.50	0.45	0.40
6	158.85	516.45	0.45	0.45